Lawrence Berkeley National Laboratory
Recent Work

Title
CRYSTALLOGRAPHIC SITE OCCUPANCY REFINEMENTS IN THIN-FILM OXIDES BY CHANNELLING ENHANCED MICRQANALYSIS

Permalink
https://escholarship.org/uc/item/0dx5t8rr

Authors
Krishnan, K.M.
Rez, P.
Thorns, G.

Publication Date
1984-07-01

eScholarship.org Powered by the California Digital Library
University of California

UC-25

LBL-18128
Preprint c.1

Lawrence Berkeley Laboratory
UNIVERSITY OF CALIFORNIA

Materials & Molecular Research Division

RECEIVED
LAWRENCE
BERKELEY LABORATORY
AUG 20 1984
LIBRARY AND
DOCUMENTS SECTION

Submitted to Acta Crystallographica

CRYSTALLOGRAPHIC SITE OCCUPANCY REFINEMENTS IN THIN-FILM OXIDES BY CHANNELLING ENHANCED MICROANALYSIS

K.M. Krishnan, P. Rez, and G. Thomas

For Reference
Not to be taken from this room

July 1984

Prepared for the U.S. Department of Energy under Contract DE-AC03-76SF00098

LBL-18128 c.1

DISCLAIMER

This document was prepared as an account of work sponsored by the United States Government. While this document is believed to contain correct information, neither the United States Government nor any agency thereof, nor the Regents of the University of California, nor any of their employees, makes any warranty, express or implied, or assumes any legal responsibility for the accuracy, completeness, or usefulness of any information, apparatus, product, or process disclosed, or represents that its use would not infringe privately owned rights. Reference herein to any specific commercial product, process, or service by its trade name, trademark, manufacturer, or otherwise, does not necessarily constitute or imply its endorsement, recommendation, or favoring by the United States Government or any agency thereof, or the Regents of the University of California. The views and opinions of authors expressed herein do not necessarily state or reflect those of the United States Government or any agency thereof or the Regents of the University of California.

(To be submitted to Acta Cryst.)

CRYSTALLOGRAPHIC SITE OCCUPANCY REFINEMENTS IN THIN-FILM OXIDES BY CHANNELLING ENHANCED MICROANALYSIS

Kannan M. Krishnan, Peter Rez* and Gareth Thomas

National Center for Electron Microscopy

Lawrence Berkeley Laboratory

University of California

Berkeley, CA 94720

*Present address: VG Scientific Ltd., Imberhorne Lane, East Grinstead, W. Sussex, RH1914B, England

ABSTRACT

Specific site occupation determinations of rare earth additions in thin film garnets of nominal composition $Y_{1.7}Sm_{0.6}Lu_{0.7}Fe_5O_{12}$ based on the orientation dependence of electron-induced characteristic x-ray emissions is described. The application of this technique called "Channelling Enhanced Microanalysis" to a general non-layered crystal structure, requires a theoretical prediction of the characteristic x-ray production as a function of incident beam orientation because the specific site sensitive orientations cannot be determined by inspection of the crystal structure. Hence, a real space formulation considering flux loss from the incident beam and under the assumption of highly localized inner shell excitations has been described for the characteristic x-ray production in thin crystals. Applying this theory, a $\bar{g} = 1\bar{2}1$ systematic orientation was predicted to be the orientation that is specific site sensitive for these thin film garnets. Experimentally observed data were then refined, using a constrained least squares analysis to give probabilities for the occupation of RE additions in the different crystallographic sites. Thus, it has been shown that in these compounds, Lu^{3+} and Sm^{3+} additions prefer octahedral occupation with a probability $\geq$ 95%. Assumptions, limitations and future potentials of this novel crystallographic technique are also discussed.

1. Introduction

The anomalous transmission of x-rays, incident on a single crystal oriented close to the Bragg position was first observed by Borrman (1941) and later interpreted by von Laue (1949) in terms of the standing wave patterns set up in the crystal by the incident x-ray beam as it propagates along specific crystal directions. It was argued that the intensity modulation of the primary beam within the crystal is such that it is a maximum on the crystallographic sites for certain incident beam orientations. For these orientations an accompanied increase in anomalous absorption and an enhancement of the secondary

emissions arising from highly localized scattering events will result. For other orientations, the intensities are a minimum on these crystallographic sites with a concomitant reduction in absorption and emission products. Similar anomalous transmission effects of the primary beam have been observed in electron diffraction patterns (Honjo, 1953; Honjo and Mihama, 1954) and also used in the interpretation of electron micrographs (Hashimoto, Howie and Whelan, 1960; Hashimoto, Howie and Whelan, 1962).

The primary absorption process for x-rays is the photoelectric effect. The inelastic scattering processes that lead to the attenuation of an electron beam in single crystals are quite different and a proper understanding of the same would involve a more detailed theory and some calculations (Heidenreich, 1962; Humphreys and Hirsch, 1968; Radi, 1969). Even though the related process of inner shell ionization does not lead to any significant attenuation in electron diffraction, the resultant electron-induced characteristic x-ray emissions are convenient, as they can be used to monitor these attenuations. Hirsch, Howie and Whelan (1962) suggested that these electron-induced characteristic x-ray emissions might also be dependent on the orientation of the incident beam with respect to the crystal, i.e. the "Borrman effect" might apply for the emission product. This was indeed observed by Duncumb (1962). However, the first experimental observation of the orientation dependence of the emission product was made by Knowles (1956) who used an incident neutron beam to excite x-ray emissions. The electron-induced characteristic x-ray emissions were further investigated by Hall (1966) who confirmed that the "Borrman effect" was only of importance for thin crystals ($t \leq 2000Å$). Finally, Cherns, Howie and Jacobs (1973) have developed a theoretical formalism to describe this phenomenon and have discussed its ramification on conventional x-ray microanalysis in great detail.

Cowley (1964) made the first suggestion that it should be possible to derive structural information from measurements of x-ray fluorescence radiation given by atoms within a diffracting crystal. The positions of solute atoms in a crystalline lattice were

experimentally determined by the nature of their x-ray fluorescence during a diffraction process by Batterman (1969). The structural information in diffuse inelastic scattering of electrons has been examined theoretically by Gjonnes and Hoier (1971). More recently, an experimental technique for locating atom positions called "Atom Location by Channelling Enhanced Microanalysis (ALCHEMI)" has been developed by Spence and Tafto (1983) and applied to a number of simple and ideal crystal structures (Tafto, 1982; Tafto and Lilienthal, 1982; Tafto and Spence, 1982a; Tafto and Spence, 1982b). A theoretical generalization of the technique of ALCHEMI has been derived (Krishnan and Thomas, 1984) and the application of this generalized formulation has been demonstrated (Krishnan, Rabenberg, Mishra and Thomas, 1984). However, applications of this technique to site-occupancy studies in complicated crystal structures require an alternative formulation and approach (Krishnan, Rez, Mishra and Thomas, 1983). This is the subject that is addressed in this paper.

2. The Technique: Physical description

The characteristic x-ray spectrum produced by the interaction of fast electrons with a crystalline specimen shows significant variation with the orientation of the incident beam. This is best illustrated in Fig. 1. One usually uses a fixed electron source, a fixed detector whose position with respect to the specimen is specified by the take-off angle (ψ) and a thin foil specimen, whose orientation (θ) can be changed precisely by the use of a goniometer, such that the orientation of the incident beam with respect to the specimen is well determined (Fig. 1a). One observes that the characteristic x-ray spectra change with incident beam orientations; there is a change in the intensities of individual peaks but the peak positions themselves do not change as they correspond to fixed atomic transitions. Hence, under certain favourable orientations, the spectra arising from beams channelled between specific planes when compared with those arising from beams blocked by the same set of planes can be used to obtain a chemical microanalysis of those planes. This is termed channelling enhanced microanalysis (CEM).

However, it has already been shown that for certain systematic or "planar channelling" conditions, the characteristic x-ray emissions induced by the channelling or blocking of the incident electrons can provide information on the occupancy of specific crystallographic sites by different elements, provided that an a priori knowledge of the distribution of some reference elements in the host lattice is available (Tafto, 1979; Spence and Tafto, 1983). In this formulation either the enumeration of parameters such as absorption coefficients, specimen thickness, etc. or an a priori knowledge of the dynamical wave function in the crystal is eliminated by a judicious choice of the reference elements. The distribution of the impurity or alloying elements is then determined by an elegant method of ratios of their characteristic x-ray intensities with respect to those of the reference elements (Spence and Tafto, 1983). This is particularly applicable to crystals with a layered structure (i.e. crystals that in some crystallographic projections can be resolved into alternating layers of parallel non-identical planes [A,B,A,B,...], each plane containing one or more specific crystallographic site) where the appropriate systematic orientation can be determined by mere inspection (Figs. 2A and 2B). For example, the spinel structure compounds can be resolved in the [001] projection into alternating planes of tetrahedral and octahedral sites and hence a $\bar{g} = 400$ systematic orientation can be easily seen to be appropriate for this kind of experiment. In many practical alloys/compounds it might not be possible to choose reference elements that are uniquely distributed on one and only one of the two alternating crystallographic planes (Fig. 2B). Further the alloying concentrations might be large enough to alter the distributions of the constituent elements in the original compound, thereby invalidating the practice of using the original compounds as internal reference standards. In such cases a more comprehensive analysis incorporating the stoichiometry of the original compound is required (Krishnan and Thomas, 1984; Krishnan, Rabenberg, Mishra and Thomas, 1984).

If the crystal structure is not a layered one (Fig. 2C), then it is not obvious by mere inspection which systematic orientation is specific site sensitive. In such cases, the

electron induced characteristic x-ray emission intensities for different site occupations and different incident beam directions have to be calculated. From these calculations the appropriate systematic or planar channelling condition applicable to that particular crystal structure is determined and the experiment performed.

3. Theory of electron-induced characteristic x-ray emissions

Ionizations of inner shell electrons alter the imaginary part of the crystal potential and this could be calculated from the relevant wave functions (Whelan, 1965a). The incorporation of an imaginary crystal potential $iP(\underline{r})$ in the Schrodinger equation, has been shown by Heidenreich (1962) to lead to a rate of electron loss per unit volume at the point $\underline{r}$ proportional to $P(\underline{r})\ |\phi(\underline{r})|^2$. When an imaginary potential is introduced, the Schrodinger equation is written as

$$\nabla^2\phi + \frac{2m}{\hbar^2}(E + V + iP)\phi = 0 \qquad (1)$$

and following Heidenreich (1962) it can be shown that the rate of "absorption" of electrons in a volume V is given by

$$\frac{m}{hk}\int \overline{\nabla}.\overline{S}\, d^3r = \frac{2m}{\hbar^2}\int P(\overline{r})\ |\phi(\overline{r})|^2 d^3r \qquad (2)$$

This could equal the rate of x-ray production if and only if $P(\underline{r})$ is chosen appropriately.

Since the absolute magnitude of the effect is unimportant for our purposes, we have assumed this imaginary part of the crystal potential to be a delta function at the mean atomic positions, i.e., a highly localized scattering process.

Therefore, the rate of characteristic x-ray production for the element "Z" given by (equation 2)

$$N_Z = \int P(\bar{r}) \; |\phi(r)|^2 \, d^3r \tag{3}$$

where the integral extends over the volume of the crystal, can be reduced under the above approximation to

$$N_Z = \sum_{RSI} \int_0^t \phi^* \phi \, dz \; . \tag{4}$$

Here ϕ is the scattered wave amplitude at any depth z expressed as a linear combination of Bloch waves, for the case of an incident plane wave, in the conventional dynamical theory formulation and the summation is over the relevant crystallographic sites of interest [RSI] where the particular element Z is distributed in the unit cell.

The excitation amplitudes ψ^i and the wavevectors k^i of the Bloch waves are perfectly well defined being dependent only on the crystal orientation and the potential. Hence

$$\int_0^t \phi^* \phi dz = \sum_{g,h} \exp[i(\bar{h}-\bar{g}).\bar{r}] \sum_{\substack{j,\ell \\ j=\ell}} C_o^{j^*} C_g^{j^*} C_o^{\ell} C_h^{\ell} t + \sum_{\substack{j,\ell \\ j\neq\ell}} C_o^{j^*} C_g^{j^*} C_o^{\ell} C_h^{\ell} \frac{\sin[(k_z^{\ell} - k_z^{j})t]}{k_z^{\ell} - k_z^{j}} \; . \tag{5}$$

Dividing throughout by the crystal thickness, t and summing over the specific sites where the element of interest is distributed within the unit cell, we get the following expression for the site-specific intensity per unit thickness for the characteristic x-ray production

$$N_Z = \sum_{RSI} \sum_{g,h} \exp[i(\bar{h} - \bar{g}).\bar{r}] \sum_{\substack{j,\ell \\ j=\ell}} C_o^{j^*} C_g^{j^*} C_o^{\ell} C_h^{\ell} + \sum_{\substack{j,\ell \\ j\neq\ell}} C_o^{j^*} C_g^{j^*} C_o^{\ell} C_h^{\ell} \frac{\sin[(k^j - k^{\ell})t]}{[(k^j - k^{\ell})t]} \tag{6}$$

where C_h^j are the Bloch wave coefficients and k_z^j are the components of the wave vector for the electrons in the conventional dynamical theory of electron diffraction in thin crystals (Hirsch, Howie, Nicholson, Pashley and Whelan, 1965). For a centrosymmetric crystal, the Bloch wave elements C_h^j and the excitation amplitudes ψ^i can be taken as real. This expression (6) for the characteristic x-ray production is composed of two parts; a thickness independent term of individual Bloch wave contributions and a thickness dependent term of Bloch wave interference contributions.

This real space formulation derived by considering the flux loss from the initial beam is consistent with the reciprocal space formulation of Howie (1963) which was derived by applying first order perturbation theory to the inelastically scattered state, i.e. the imaginary part of the crystal potential in Yoshioka's (1957) formulation was considered to be small. The crucial step in the argument is that for highly localized inner shell excitations where the inelastic potential is well approximated by a delta function $\delta(r)$, the Fourier transform P_{gh} is a constant and does not appear explicitly in equations (5) and (6).

4. Results of the characteristic x-ray production calculations at 100kV

In this section, the results of the calculation of the orientation dependence of electron-induced characteristic x-ray production at an accelerating voltage of 100kV are presented for two compounds: $MgAl_2O_4$ (spinel) and the prototype garnet compound $Y_3Fe_5O_{12}$.

The normal spinel structure is a layered one, for it can be resolved in the [100] projection into alternating (400) planes of octahedrally coordinated Al atoms with tetrahedrally coordinated Mg atoms distributed mid-way between them (Fig. 3). Hence, the x-ray intensities for Mg and Al in a normal spinel were calculated for a 15-beam ($-7\bar{g}$ to $+7\bar{g}$), $\bar{g}$ = 400 systematic excitation condition and over a range of incident beam orientations. The orientation of the incident beam was specified by varying the values of the excitation error k_x/g which is defined such that k_x/g = 0.5 for the exact first order Bragg diffraction

condition. Figure 4 shows the results of the calculations. It can be seen that the standing wave is localized on the tetrahedrally coordinated Mg atoms for positive excitation errors ($k_x g/ > 0.5$) and on the octahedrally coordinated Al atoms for negative excitation errors ($k_x/g < 0.5$) of the first order Bragg diffraction condition with a correspondingly enhanced characteristic x-ray production.

This predicted orientation dependence of the characteristic x-ray emissions is in good agreement with the experimental results of Tafto and Spence (1982a) for spinels. This served as a verification for the validity of the theoretical formulation.

The garnet structure with an average chemical formula of $\{A_3^{2+}\}\ [B_2^{3+}](Fe_3)O_{12}$ is very much more complicated. It belongs to the space group $I\frac{4_1}{a}\ 3\frac{\bar{2}}{d}(O_h^{10})$ with a typically large lattice parameter ($a_o = 12.376 \pm 0.004Å$). It is not possible by mere inspection of the crystal structure (Fig. 5) either to say whether it is layered or to identify crystallographic planes where a particular site is predominant. All that which can be inferred from a close inspection of a series of projections of this crystal structure generated by Bennemma and Giess (1981) using the ORTEP (Johnson, 1965) computer graphics program is that it is possible in the [100] projection to isolate the octahedral [a] sites from the others for in this projection the (008) planes are alternately endowed with these octahedral [a] sites.

Therefore, x-ray emission intensities were calculated for complete rare earth occupation in any one of the three crystallographic sites of the prototype compound YIG for different systematic excitation conditions (i.e., $\bar{g} = 00\bar{2}$, $\bar{g} = \bar{2}20$, $\bar{g} = 1\bar{2}1$ etc.) to determine an orientation with specific-site sensitive characteristic x-ray emissions. These 11-beam calculations, for systematic excitation conditions ($-5\bar{g}$ to $+5\bar{g}$) were performed for a range of crystal thicknesses (250Å - 2000Å) and for a range of incident beam orientations ($0 < k_x/g < 2$). The x-ray production was found to be insensitive to crystallographic orientations, irrespective of the site occupation, for excitations of the $\bar{g} = 00\bar{2}$ and $g = \bar{2}20$ systematic diffraction conditions. On the other hand, a strong orientation dependence for the $\bar{g} = 1\bar{2}1$

systematic excitation condition was predicted at the exact first order Bragg diffraction conditions ($k_x/g = 0.5$) and for negative and positive excitation errors (Fig. 6), i.e., channelling for dodecahedral site substitutions of the rare earth additions, blocking for tetrahedral substitutions and an insensitivity to orientation for octahedral substitutions.

5. Experimental details

5.1. Specimen preparation

Samples of nominal melt composition $Y_{1.7}Sm_{.6}Lu_{.7}Fe_5O_{12}$, 0.94μm thick, grown on GGG substrates by liquid phase epitaxy, at a growth temperature of 969°C and a growth rate of 1.76 μm/min, were studied. Details of the preparation of these samples (liquid phase epitaxial growth), which were supplied by Bell Labs, are given elsewhere (Mathews, 1975).

Thin foils of these samples for observation in a transmission electron microscope (TEM) equipped with an energy dispersive x-ray (EDX) detector were prepared by the routine ion milling technique. However, some minor changes in the case of these LPE grown thin films were introduced. Ultrasonically cut disks of 3mm diameter were mechanically thinned to a thickness of 35-50 microns (determined by optical microscopy) and then milled with argon ions from the side of the substrate only. An acceleration voltage of 6-8kV, a specimen current of approximately 20 microamps and an incidence angle of 18° were the normal milling conditions. This gave a very thin electron transparent region of the film. However, some surface pitting and damage were observed at this stage and were eliminated by cleaning the specimen in an ion-milling machine using Ne (a lower atomic weight inert gas) ions at reduced acceleration voltages. In fact, this problem could altogether be avoided by using the latter as the milling medium, even though this is a considerably slower and time consuming process.

The garnet films grown on the substrates are subjected to residual strains because of the slight mismatch of the cooling rates between the film and substrate. On ion milling, the lack of the substrate support caused many of the films to buckle rendering them useless

for TEM observations. This persistent limitation of the specimen preparation technique could not be avoided by any systematic procedure, but could only be circumvented by preparing a large number of specimens.

5.2. Analytical and Transmission Electron Microscopy

Experiments were performed on a Philips 400ST analytical transmission electron microscope fitted with a LaB_6 filament and an EDAX energy dispersive analyser. The detector configuration was such that the maximum x-ray collection was achieved for a take-off angle of 20° (a specimen tilt of 10° towards the detector). A low background double tilt specimen holder to reduce x-ray background was used in all experiments. Stray x-ray generation was further minimized by using gridless self supporting specimens. The specimen thicknesses were estimated by convergent beam electron diffraction (CBED) to be approximately 50nm. The incident beam divergence was a few milliradians and the probe diameter was 50-100nm. The latter is determined by the level of contamination. The characteristic x-ray emissions were collected at different orientations of the collimated electron beam based on the calculations described earlier. A strong $\bar{g} = 1\bar{2}1$ systematic row was excited and spectra collected at six different orientations of the incident electron beam:

(1) Symmetric orientation; $k_x/g = 0$

(2) First order Bragg diffraction with small negative excitation error ($s < 0$); $k_x/g \simeq 0.375$

(3) Exact first order Bragg diffraction; $k_x/g = 0.5$

(4) Small negative deviation from the second order Bragg diffraction; $k_x/g \simeq 0.875$.

(5) Exact second order Bragg diffraction; $k_x/g = 1.0$

(6) Second order Bragg diffraction with small positive deviation parameter; $k_x/g \simeq 1.125$.

The specimens were oriented in all experiments using either convergent beam electron diffraction or the Kikuchi line method.

In order to ensure proper statistics, spectra were collected (at the appropriate orientations) for a total counting time of 600 seconds and a counting rate of ~3000 counts/sec. A hole count was taken at periodic intervals and substracted along with the continuous background from the spectra.

6. Experimental results

The integrated intensities for the two rare earth additions of interest, Sm and Lu, after substraction of the continuous background, at the orientations mentioned earlier are shown in Table 1. Because of the large counting time (600 secs) and the susceptibility of the specimen to damage and contamination, the spectra were collected at a different specimen sampling area for each orientation of the incident electron beam (specimen tilt). Care was taken to ensure that the specimen thickness was not significantly different for the different acquisitions. However, small differences in counting rates or changes due to the small displacements of the probe had to be incorporated in the analysis. This was done by scaling the integrated elemental intensities (Table 1) using scaling factors that are actually normalized ratios of the total integrated intensities of the whole spectra (Table 2). This gave the normalized integrated elemental intensities for the two rare earth additions (Table 3). The standard deviations ($\sqrt{N}$) of the observations are ~0.5% and ~0.60% for Lu(L_α) and Sm(L_α) respectively.

The data is statistically significant but a clear agreement with the theoretical predictions for complete substitutions of the rare earth additions in any particular crystallographic site is not obviously evident. This was interpreted to be due to a mixed distribution of the rare earth additions in all the possible crystallographic sites. The probabilities were then determined by a least squares refinement based on the algorithm of constrained least squares by Lawson and Hanson (1974).

Table 1

Integrated Elemental Intensities

k_x/g	0	0.375	0.5	0.875	1.0	1.125
$Lu(L_\alpha)$	57061	51324	61452	50142	60061	59541
$Sm(L_\alpha)$	35839	32761	39785	32073	38277	37546

Table 2

Scaling Factors

k_x/g	0	0.375	0.5	0.875	1.0	1.125
Total Counts	1606095	1475254	1788690	1429993	1753256	1688060
Scaling Factor	1.1231	1.0317	1.2508	1.0000	1.2261	1.1805

Table 3

Normalized Integrated Elemental Intensities

k_x/g	0	0.375	0.5	0.875	1.0	1.125
$Lu(L_\alpha)$	50807	49747	49130	50142	48985	50437
$Sm(L_\alpha)$	31911	31754	31808	32073	31218	31805

The standard deviations of these observations are 0.5% and 0.60% for $Lu(L_\alpha)$ and $Sm(L_\alpha)$ respectively.

7. Analysis

7.1 Least squares refinement

The integrated elemental intensity was calculated as a summation over all sites of the product of the theoretical value for complete occupation of each site and a weight factor representing the probability of occupation of that specific site. Mathematically this is expressed as

$$I_\eta^Z = K_\eta \sum_\alpha B^Z(\eta,\alpha) p_\alpha^Z \tag{7}$$

where

$B^Z(\eta,\alpha)$ -Calculated integrated intensity for the element Z at the specific orientation η and the complete occupation of the specific site α.

p_α^Z -Weight of occupation of site α by the element Z to be determined by the refinement. However, the refinement is subject to the constraint $p_\alpha^Z \geq 0$, for every α and Z.

K_η -Scaling factor for the particular orientation η.

I_η^Z -Theoretical estimate of the experimentally observed integrated intensity of element Z for the specific orientation η.

Then an error term was defined as the difference between the experimentally observed intensity and the theoretical estimate obtained above. For each element of interest, i.e. Sm and Lu, the least squares problem with inequality constraints can be stated as the min-

imization of a summation over all orientations of the square of this error term, subject to the constraint that all the weights are positive. That is, minimize

$$\mathcal{J}^Z = \sum_\eta \left(\frac{X_\eta^Z}{K_\eta} - \frac{I_\eta^Z}{K_\eta} \right)^2 \tag{8}$$

subject to

$$p_\alpha^Z \geq 0 \text{ for every } \alpha \text{ and } Z \ .$$

Here X_η^Z/K_η are the experimentally observed integrated intensities scaled as described earlier for element Z and orientation η .

Introducing the differential operator δ we obtain the following condition for the minimum:

$$\delta\,(\mathcal{J}^Z) = 0 \tag{9}$$

which gives the following matrix equations

$$\underline{\underline{M}}^Z \underline{P}^Z = \underline{V}^Z \tag{10}$$

with their components given by

$$V_\alpha^Z = \sum_\eta X_\eta^Z B^Z(\eta,\alpha) \tag{11}$$

and

$$M_{\alpha,\beta}^Z = \sum_\eta B^Z(\eta,\alpha)\, B^Z(\eta,\beta) \ . \tag{12}$$

Hence

$$\underline{P}^Z = (\underline{\underline{M}}^Z)^{-1} \underline{V}^Z . \tag{13}$$

Applying this least square analysis to the data in Table 3 for the observed characteristic x-ray intensities and refining it with respect to the intensities calculated using the theory developed earlier, the weights of the occupation for each of the two rare earth additions were obtained (Table 4).

Table 4

Relative weights for the site occupancy of the RE additions

	Octahedral	Tetrahedral	Dodecahedral	RNORM $\|\|\underline{\underline{M}}\underline{P} - \underline{V}\|\|$
Lu	0.2141 $\pm$ 0.02	0.0049 $\pm$ 0.005	***	7.778×10^{-4}
Sm	0.1679 $\pm$ 0.0164	***	0.0095 $\pm$ 0.0007	4.006×10^{-3}

Within the limitations of the assumptions of the technique, it can be inferred that the substitution of these rare earth additions in the octahedral sites of this crystal structure is highly probable, with a probability $\geq 95\%$. These results are in good agreement with earlier studies (Suchow and Kakta, 1972; Blank, Nielsen and Biolsi, 1976), particularly for the distribution of the small rare-earth ion, Lu^{3+} which can easily be accommodated in the smaller octahedral site.

7.2. Error analysis

Let the error in the observed spectra be $\Delta X_\eta = 3\sigma = 3\sqrt{X_\eta}$ where σ is the standard deviation of the experimental observation. The errors in this analysis were calculated in quadrature. Hence, the components of the right array $\underline{V}^Z$ in the matrix equation

$$\underline{\underline{M}}^Z \underline{P}^Z = \underline{V}^Z \tag{14}$$

would be given by

$$V_\alpha^Z \pm \Delta V_\alpha^Z = \sum_\eta [X_\eta^Z B^Z(\eta,\alpha)] \pm \sqrt{\sum_\eta 3\,\Delta X_\eta^Z [B^Z(\eta,\alpha)]^2}\ . \tag{15}$$

The errors in the weights of occupation of the different crystallographic sites for the two RE additions were then determined by carrying out the least squares analysis for the upper and lower bounds of the values of X_η^Z, i.e. $X_\eta^Z + \Delta X_\eta^Z$ and $X_\eta^Z - \Delta X_\eta^Z$ respectively.

Finally the credibility of the least squares refinement was established by determining the norm, i.e. $R = \|\underline{\underline{M}}\,\underline{P} - \underline{V}\|$ (RNORM in Table 4) and ensuring that this was less than some acceptable value ($\leq 10^{-2}$).

8. Discussion

The single most important assumption in this formulation is that the associated inner shell excitations are highly localized (to the point of being approximated by delta functions at the mean atomic positions) when compared with thermal vibrations. This assumption has been made in light of the following arguments.

Gjonnes and Hoier (1971) have estimated the "radius" of 1s orbitals to be approximately 0.02Å using electronic band structure calculations, i.e. "the probability density for the 1s electron in a medium or heavy atom is so narrow that any distribution associated with the K-shell will also be narrow". Bourdillon, Self and Stobbs (1981) have used an alternative approach, estimating the time τ over which a virtual photon is exchanged between a fast electron and the excited particle and converting that (following Howie, 1979), using the uncertainty principle, to give an expression for the limiting value of the impact parameter, b. Using a number of radically simplifying arguments they have shown that an expectation value for the impact parameter can be computed as

$$\langle b \rangle = 1.24\hbar\, v/4.46E_c \tag{16}$$

where E_c is the initial energy for the onset of the transition. The value of the impact parameter, calculated using the above expression for the values of the energy loss relevant to the characteristic x-ray emission for the elements of interest, are shown in Table 5.

These values of the impact parameter along with the values obtained from electronic structure calculations suggest that the approximation is indeed a reasonable one.

Table 5

Calculated expectation values of
the impact parameter

Emission	E_c(keV)	$\langle b \rangle$(nm)
Al(K_α)	1.486	0.0231
Mg(K_α)	1.253	0.0274
Fe(K_α)	7.019	0.0049
Sm(L_α)	6.656	0.0068
Lu(L_α)	9.281	0.0037

A source of inelastic scattering not included in the theory is phonon scattering. This highly localized scattering event with significant contributions to anomalous absorption has been treated by a number of different authors (Takagi, 1958a; Takagi, 1958b; Whelan, 1965b; Hall and Hirsch, 1965). The simplest treatment is to calculate Bragg scattering by modifying the scattering factors as $f(g)\exp[-\alpha(g)]$ where $\alpha(g)$ is the accepted Debye-Waller factor. These thermal vibrations could be incorporated (Cherns, Howie and Jacobs, 1973; Otsuki, 1966) by considering that the region of x-ray production is approximated by a delta function broadened by thermal vibrations such that the imaginary part of the crystal potential $P(r)$ has Fourier components P_g given by

$$P_g = P_o \exp(-\alpha g^2) \ . \tag{17}$$

Again this would be valid only because the localizations for inner shell excitations is much smaller than the thermal vibration amplitudes. The modified expression for characteristic x-ray emissions would then be

$$N_z = \int |\phi(r)|^2 \sum_g P_g \exp(i\bar{g} \cdot \bar{r}) d^3r \tag{18}$$

where as in equation 3 the integral would be over the volume of the crystal.

However, Cherns, Howie and Jacobs (1973) have shown that the reduction of the orientation dependent characteristic x-ray emission due to the thermal vibrations is not significant for temperature rises up to 200°C when compared with reductions due to the angular spread.

From the experimental point of view, one of the significant advantages of the use of the orientation dependence of electron induced characteristic x-ray emissions in specific site occupation studies over other accepted techniques, particularly in the studies of magnetic materials, is that this technique could be potentially applied to study local areas of the specimen; a spatial resolution of 50-100nm is quite routine. This requires the use of a convergent electron probe. The theory developed here is strictly valid for parallel illumination only. If we want to be rigorous in applying this theory to cases where convergent probes of the order of a few hundred angstroms are used, then it should be suitably modified. This should pose no difficulties and involves resorting to the accepted method (Duval, Duval and Henry, 1974; Duval and Henry, 1974) of averaging over a whole range of incident angles. Finally, by performing conventional bright field and dark field imaging, it was ensured that the specimens were defect-free.

Within the confines of the above assumptions and the limitations to be described, the technique developed here is capable of resolving adjacent elements in the periodic table and is restricted in spatial resolution to 50nm. Further, trace elemental compositions (0.2-0.3wt%) can be routinely analysed. With some care, distributions of elements in specific crystallographic sites for levels of doping equivalent to 10^{20} atoms/cm^3, can be determined. The smallest error in the fraction of the total concentration occupying a particular site is a compounded one consisting of the inherent approximations of the theoretical formulation, the statistical error in experimentation and the computational error in least squares refinements. Hence, the smallest error achievable is estimated to be $\pm 5\%$.

The technique that has been described is subject to all the limitations of conventional energy dispersive x-ray microanalysis and hence is limited to the analysis of elements with atomic number $Z \geq 11$, unless windowless or ultra-thin window detectors are employed.

As these techniques pre-suppose dynamical scattering, it is recommended that the sample be of sufficient thickness ($t = n\xi_g$, where $n \geq 1$). However, there is an upper limit of $t < 2000\text{Å}$, corresponding to the attenuation distance of the poorly transmitted Bloch waves. At distances greater than this, the electrons are diffusely scattered through small angles and effectively behave as plane waves in producing further x-rays. For very thin specimens the technique of High Resolution Microscopy (HREM) might be applied as a complementary method. Here the differences in scattering factors between the host and substitutional species might be sufficient to resolve site occupancies.

The minimum probe size is limited by the statistics of the impurity distribution. The requirement of uniform distribution places a fundamental limit on the minimum volume that can be analysed. The condition that has to be satisfied (Spence and Tafto, 1983) in order that the dynamical wavefunction is well sampled in depth is given by

$$\xi_g \, nA \geq 1$$

where n(atoms/unit vol.) is the uniformly distributed concentration, A is the projected area of the electron probe and ξ_g is the dynamical extinction distance for the reflection $\bar{g}$. This condition has been satisfied in all the studies discussed in this paper.

There are innumerable other problems of site occupation determinations in materials characterization to which the techniques of channelling enhanced microanalysis can be applied. However, each problem has be tackled separately, beginning by classifying the crystal structure into one of the two categories (layered or non-layered) that have been discussed in this work and then proceed with the appropriate analysis (Krishnan, 1984).

As pointed out earlier, the best resolution in terms of detection that can be resolved by these techniques is about 10^{20} atoms/cm^3. For many applications, particularly in semiconductor materials, it would be worthwhile to increase these detectability limits. If the limitation is due to a poor signal to background ratio then a possible solution (Wittry, 1976) is to measure the characteristic x-ray and the transmitted electron energy loss (EELS) spectra simultaneously, i.e. coincidence counting. One could run into problems as not all EELS events can give rise to a detectable EDX event. If the limitation were to be the overall counting time caused by a pile up of x-ray counts from the matrix, it has been suggested (Tafto, Spence and Fejes, 1983) that it could be avoided by using suitable filters to suppress the matrix x-ray counts.

ACKNOWLEDGEMENTS

This work was supported by the Director, Office of Energy Research, Office of Basic Energy Sciences, Materials Sciences Division of the U. S. Department of Energy under Contract No. DE-AC03-76SF00098. The specimens were obtained from Dr. V. J. Fratello of Bell Labs, New Jersey. The authors would like to thank Drs. R. Sinclair and A. Pelton for the use of the AEM facilities at Stanford, Dr. J. Taftø for the use of the AEM facilities at ASU, Dr. D. Cockayne for helpful comments and criticism and Drs. R. Mishra and M. A. O'Keefe for their comments on this manuscript.

REFERENCES

Batterman, B. W. (1969). Phys. Rev. Lett. 22, 703.

Bennema, P. and Geiss, E. A. (1981). "Garnet Structure Drawings", IBM Research Report.

Blank, S. L., Nielsen, J. W. and Biolsi, W. A. (1976). J. Electrochem. Soc. 123, 845.

Borrman, G. (1941). Phys. Z. 42, 157.

Bourdillon, A. J., Self, P. G. and Stobbs, W. M. (1981). Phil. Mag. A44, 1335.

Cherns, D., Howie, A. and Jacobs, M. H. (1973). Z. Naturfor. 28A, 565.

Cowley, J. M. (1964). Acta Cryst. 17, 33.

Duncumb, P. (1962). Phil. Mag. 7, 2101.

Duval, H., Duval, P. and Henry, L. (1974). J. de Physique 35, L169.

Duval, H. and Henry, L. (1974). C. R. Acad. Sci. Paris 278B, 331.

Gjonnes, J. and Hoier, R. (1971). Acta Cryst. A27, 166.

Hall, C. R. (1966). Proc. Roy. Soc. A295, 140.

Hall, C. R. and Hirsch, P. B. (1965). Proc. Roy. Soc. A268, 158.

Hashimoto, H., Howie, A. and Whelan, M. J. (1960). Phil. Mag. 5, 967.

Hashimoto, H., Howie, A. and Whelan, M. J. (1962). Proc. Roy. Soc. A269, 80.

Heidenreich, R. D. (1962). J. Appl. Phys. 33, 2321.

Hirsch, P. B., Howie, A. and Whelan, M. J. (1962). Phil. Mag. 7, 2095.

Hirsch, Howie, A., Nicholson, R. B., Pashley and Whelan, M. J. (1965). "Electron Microscopy of Thin Crystals", Butterworth, London.

Honjo, G. (1953). J. Phys. Soc. Jap. 8, 776.

Honjo, G. and Mihama, K. (1954). J. Phys. Soc. Jap. 9, 184.

Howie, A. (1963). Proc. Roy. Soc. A271, 268.

Howie, A. (1979). J. Microscopy 117, 1.

Humphreys, C. J. and Hirsch, P. B. (1968). Phil. Mag. 18, 115.

Johnson, C. K. (1965). ORTEP, ORNL Report No. 3794, Oak Ridge.

Knowles, J. W. (1956). Acta Cryst. 9, 61.

Krishnan, K. M., (1984). Ph.D. Thesis, University of California, Berkeley.

Krishnan, K. M., Rez, P. and Thomas, G. (1983). Proc. HVEM Conf., Berkeley, California, p. 365, eds. R. Fisher, R. Gronsky, and K. H. Westmacott.

Krishnan, K. M., Rez, P., Mishra, R. K. and Thomas, G. (1983). Proceedings on the "Electron Microscopy of Materials", Materials Research Society Symposium, Boston, Massachusetts, 31, 79.

Krishnan, K. M. and Thomas, G. (1984). accepted for publication in J. Microscopy.

Krishnan, K. M., Rabenberg, L., Mishra, R. K. and Thomas, G. (1984). J. Appl. Phys. 55, 2058.

Lawson, C. L. and Hanson, R. J. (1974). "Solving Least Squares Problems", Chapters 23 and 25, Prentice Hall, N. J.

Mathews, J. W. (1975). "Epitaxial Growth", Academic Press, N. Y.

Otsuki, Y. H. (1966). J. Phys. Soc. Jap. 21, 2300.

Radi, G. (1969). Acta Cryst. A26, 41.

Smith, D. J., Saxton, W. O., O'Keefe, M. A., Wood, G. J. and Stobbs, W. M. (1983). Ultramicroscopy 11, 263.

Spence, J. C. H. and Tafto, J. (1983). J. Microscopy 130, 147.

Suchow, L. and Kakta, M. (1972). J. Sol. St. Chem. 5, 329.

Tafto, J. (1979). J. Appl. Cryst. 15, 378.

Tafto, J. (1982). J. Appl. Cryst. 18, 452.

Tafto, J. and Lilienthal, Z. (1982). Acta Cryst. 15, 260.

Tafto, J. and Spence, J. C. H. (1982a). Ultramicroscopy 9, 243.

Tafto, J. and Spence, J. C. H. (1982b). Science 218, 49.

Tafto, J., Spence, J. C. H. and Fejes, P. (1983). J. Appl. Phys. 54, 5014.

Takagi, S. (1958a). J. Phys. Soc. Jap. 13, 278.

Takagi, S. (1958b). J. Phys. Soc. Jap. 13, 287.

von Laue, M. (1949). Acta Cryst. 2, 106.

Whelan, M. J. (1965a). J. Appl. Phys. 36, 2099.

Whelan, M. J. (1965b) J. Appl. Phys. 36, 2103.

Wittry, D. (1976). Ultramicroscopy 1, 302.

Yoshioka, H. (1957). J. Phys. Soc. Jap. 12(6), 618.

Figure Captions

Fig. 1. Physical principles of channelling enhanced microanalysis. (a) The experimental arrangement. (b) The projected crystal structure with the standing wave pattern of the primary beam set up as a result of the dynamical scattering. For a systematic orientation the wave field is two dimensional (i.e. constant in a direction normal to the page). The modulation of the standing wave on specific crystallographic planes is then a function of the incident beam orientation. (c) The characteristic x-ray emissions are a function of these modulations of the primary beam. For the favourable orientation the Bloch waves are maximized on the A-planes with a concomitant increase for the elements occupying the site Δ. For the other favourable orientation, the maximization is on the B-planes with a corresponding increase for the elements occupying the sites $\bigcirc$. By monitoring these orientation dependent emission products and resorting to the analyses to be developed in this paper, specific site occupations can be quantitatively determined.

Fig. 2. Hypothetical two-dimensional figures illustrating the classification of crystal structures in this work. $\square, \bigcirc$ - refer to the crystallographic sites of interest. The distribution of the site determines whether the crystal structure is layered (Figs. A and B) or not (Fig. C). a, b are the reference elements. If their distributions are known a priori, the simple ratio technique (A) or a generalization of the same (B) should be used. If not (C) the characteristic x-ray emissions have to be calculated and refined using a least squares refinement to determine site occupancies.

Fig. 3. A [100] projection in perspective of the spinel structure. 2 x 2 x 2 unit cells are shown. Squares represent magnesium and triangles represent aluminum. Notice that the structure is layered, i.e. in this projection it can be resolved into alternating [004] planes containing either Mg (tetrahedrally coordinated) or Al (octahedrally coordinated) ions. (Courtesy of P. Stadelman)

Fig. 4. Results of the orientation dependent x-ray emissions for spinels. A 15-beam, $\bar{g}$ = 004 systematic excitation condition (-7g to +7g) and a specimen thickness of 100Å were the conditions used. Note that there is an enhanced emission of the octahedrally coordinated Al for negative excitation error ($s < 0$) of the first order Bragg diffraction condition. The orientation dependence of the tetrahedrally coordinated Mg is reversed, i.e., an enhancement for positive excitation error ($s > 0$) of the first order Bragg reflection.

Fig. 5. Arrangements of the cations in the garnet structure. Only half the unit cell (4 formula units or 80 atoms) is shown. The oxygen ions have been removed for clarity. Note that the octahedral [a] sites form a repeating body centered cubic structure with a lattice parameter $a_0' = a_0/2$. (After Geller and Gilleo (1957).

Fig. 6. Calculated orientation dependence of the characteristic x-ray emissions of the garnet structure. An 11-beam (-5g to +5g), $\bar{g} = 1\bar{2}1$ systematic excitation condition and two thicknesses (250Å and 500Å) were the conditions used. For these conditions, it can be seen that the emission product is site sensitive, i.e., channelling for tetrahedral site substitutions, blocking for dodecahedral site substitutions and an indifference to orientation (notice change in the scale for intensity) for octahedral site substitutions of the rare earth element. Similar calculations were made for systematic excitations of other $\bar{g}$ vectors but were found to be such that the emission product is insensitive to either occupations or incident beam orientations.

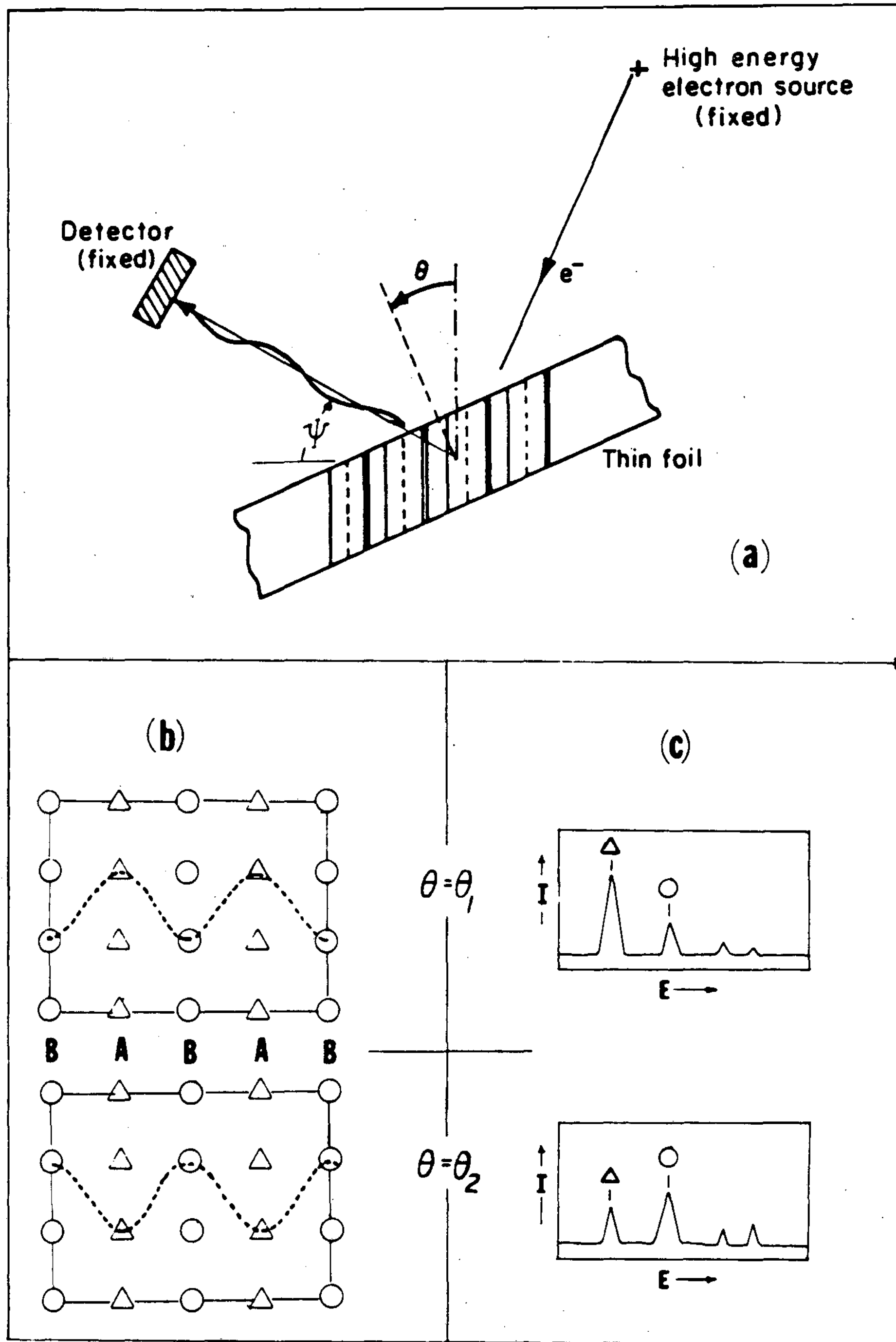

Fig. 1

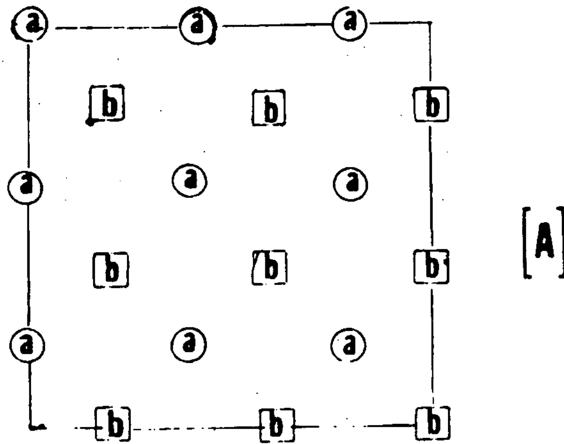

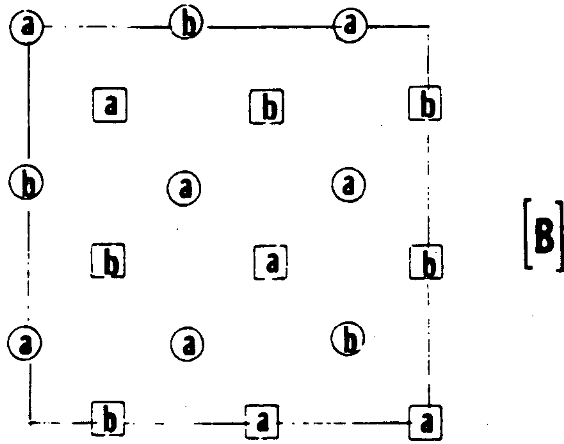

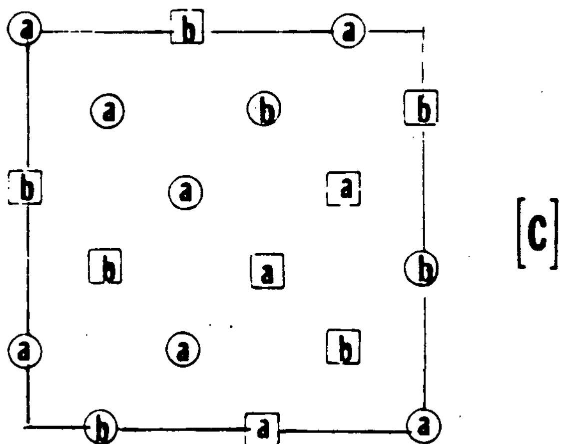

XBL 8310-12160

Fig. 2

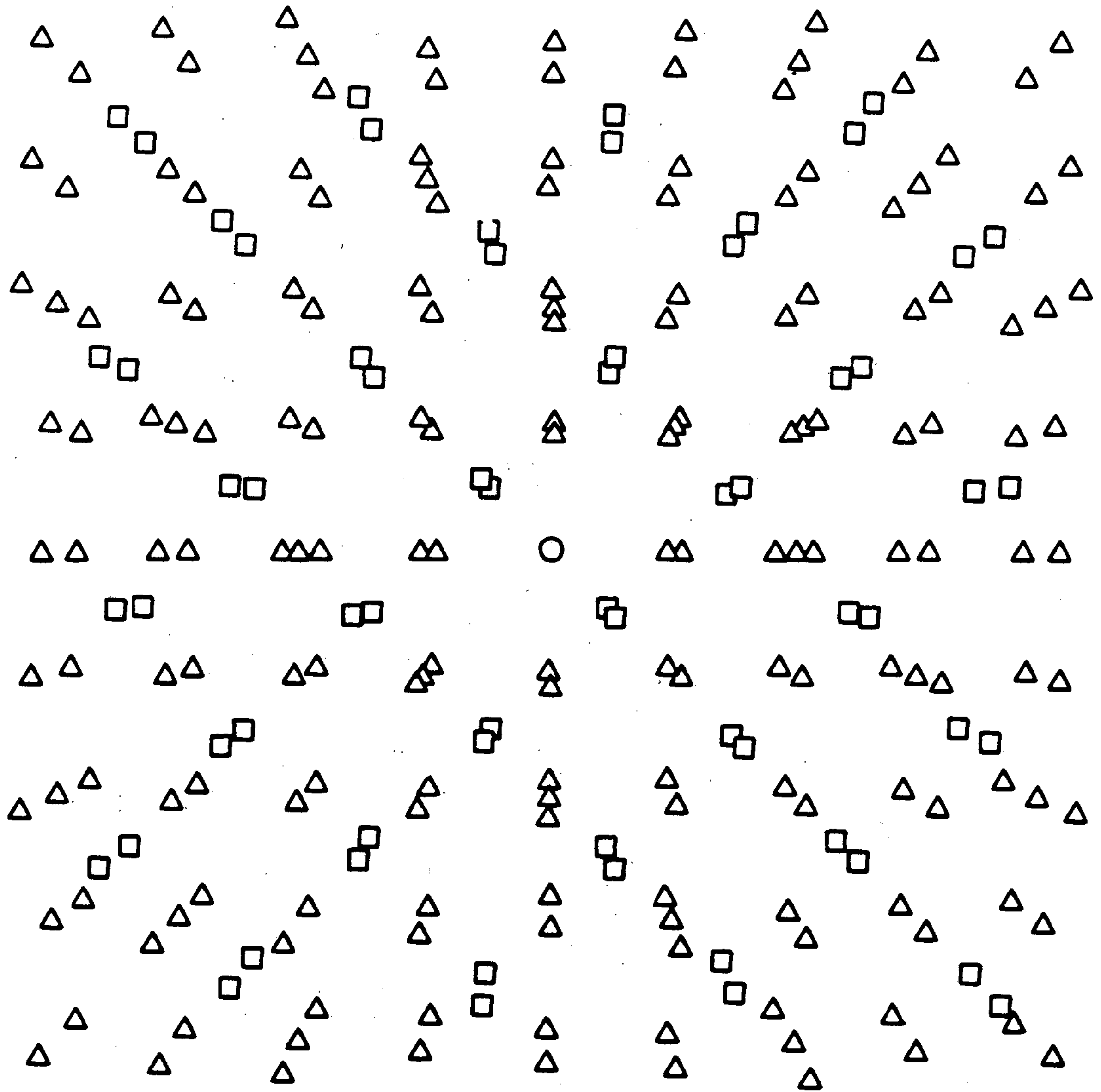

XBL 847-2866

Fig. 3

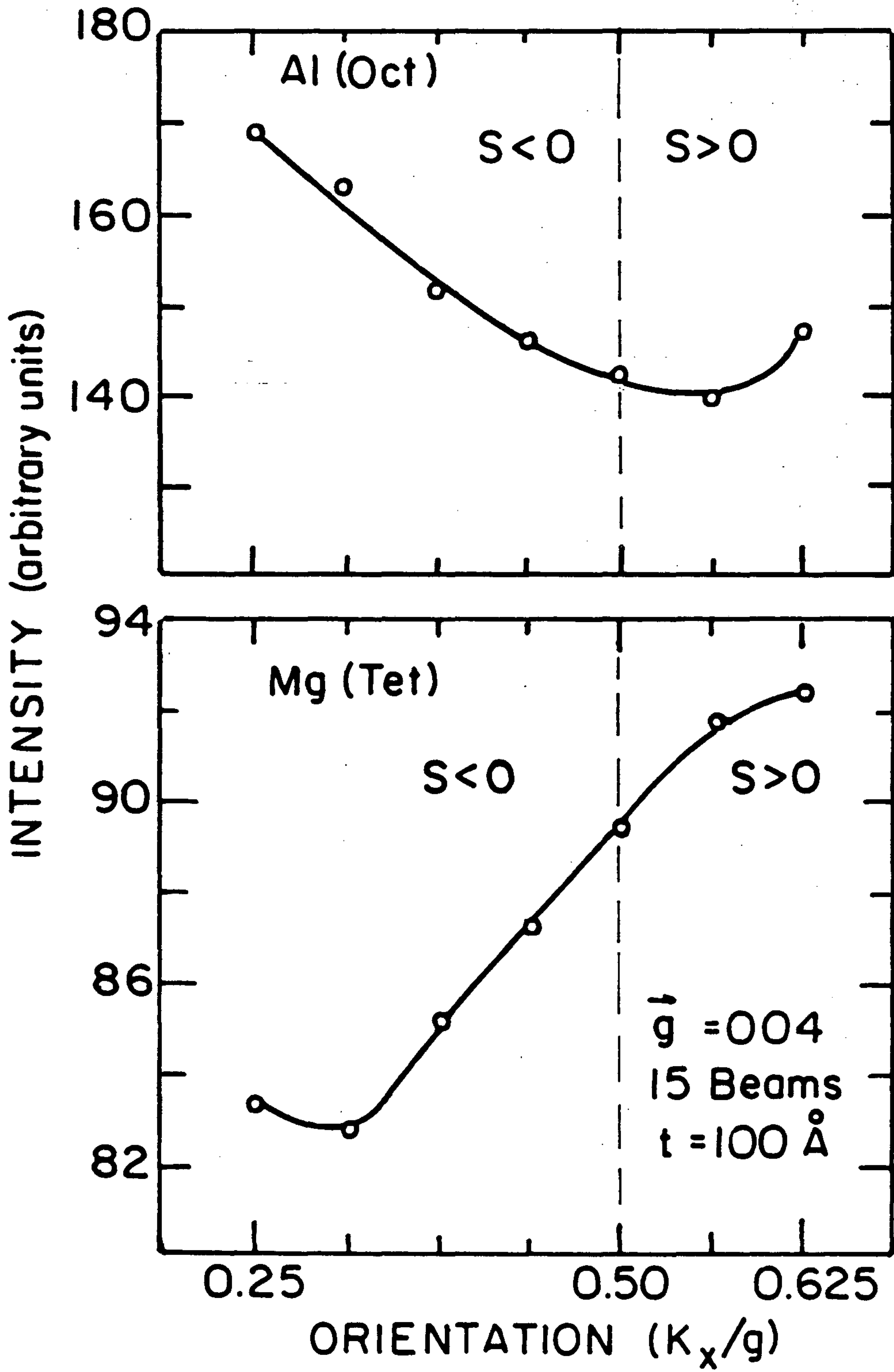

Fig. 4

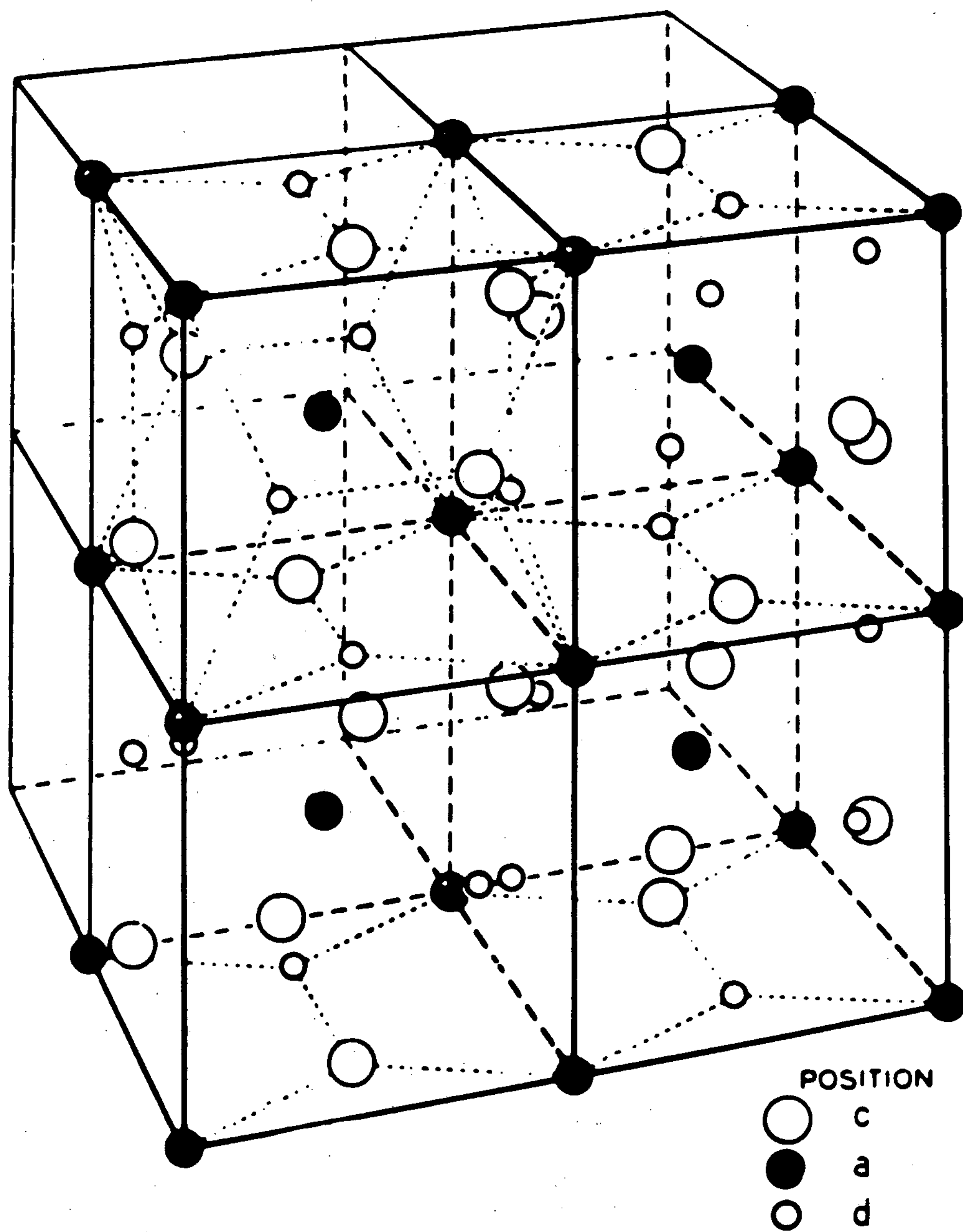

Fig. 5

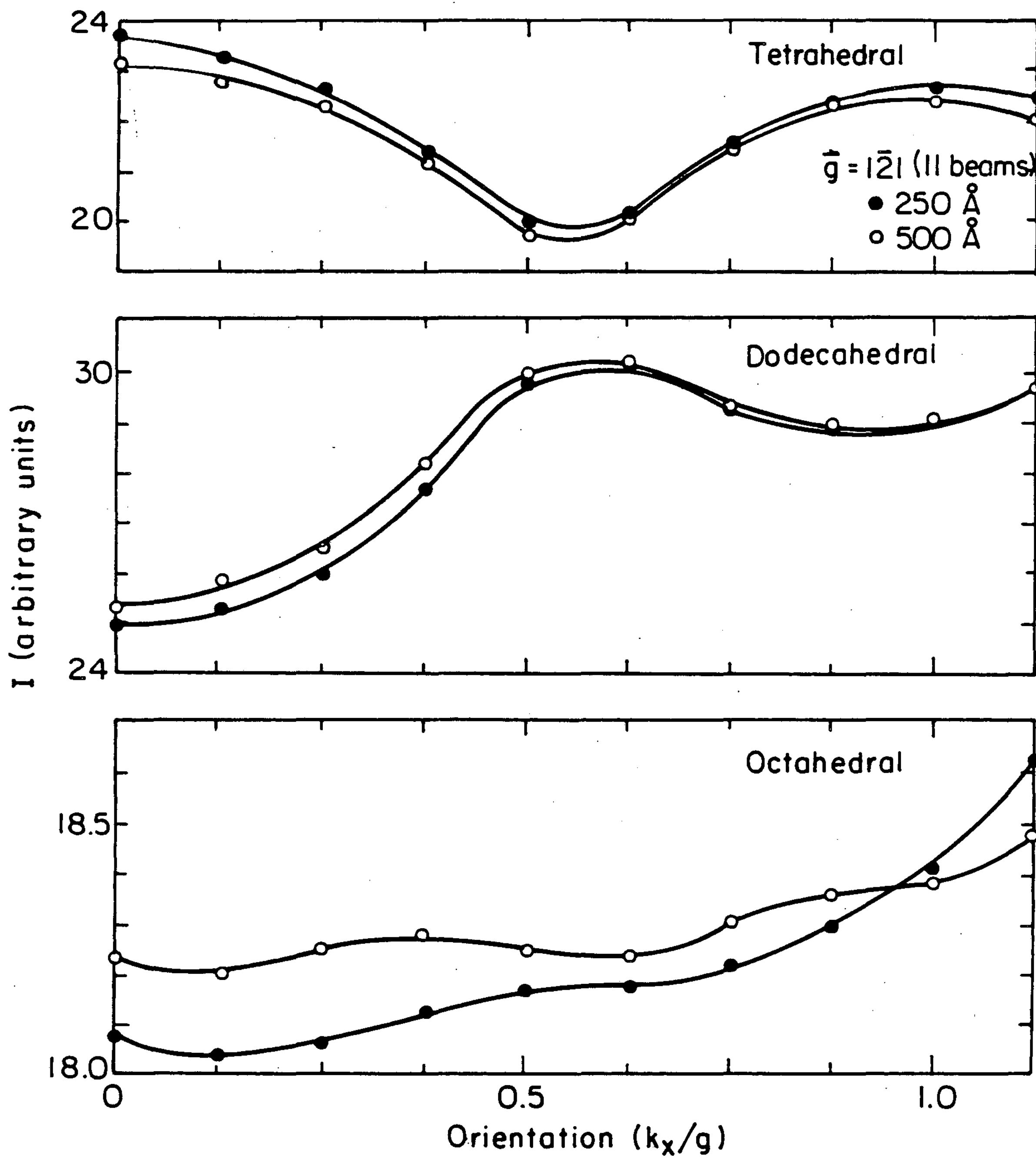

Fig. 6

This report was done with support from the Department of Energy. Any conclusions or opinions expressed in this report represent solely those of the author(s) and not necessarily those of The Regents of the University of California, the Lawrence Berkeley Laboratory or the Department of Energy.

Reference to a company or product name does not imply approval or recommendation of the product by the University of California or the U.S. Department of Energy to the exclusion of others that may be suitable.

TECHNICAL INFORMATION DEPARTMENT
LAWRENCE BERKELEY LABORATORY
UNIVERSITY OF CALIFORNIA
BERKELEY, CALIFORNIA 94720